Arab J Sci Eng (2018) 43:1435–1443
https://doi.org/10.1007/s13369-017-2965-5

RESEARCH ARTICLE - MECHANICAL ENGINEERING

Effect of Graphene Nanoplatelets and Paraffin Oil Addition on the Mechanical and Tribological Properties of Low-Density Polyethylene Nanocomposites

A. El-Sayed M. Hassan[1] · Alaa I. EiD[2] · M. El-Sheikh[1] · W. Y. Ali[3]

Received: 4 March 2017 / Accepted: 8 November 2017 / Published online: 15 November 2017

Abstract Polymeric nanocomposite materials have solved many problems due to their extensive applications such as aerospace, automobiles, coatings, and packaging materials. Low-density polyethylene (LDPE)/graphene nanoplatelets (GNPs) impregnated by paraffin oil (PO) were fabricated by a hot compression technique. Elastic modulus was calculated by results of compression test that conducted on the testing nanocomposites using a universal testing machine. Microhardness of LDPE and its composites was measured by Vickers microhardness testing machine. Tribological properties of LDPE and its composites were investigated by pin-on-disc tester at 20 N normal load, 1.2 ms^{-1} sliding velocity, and 212 m sliding distance. The results showed that the elastic modulus and microhardness of LDPE/GNP nanocomposites are higher than that of pure LDPE and then gradually decreased by adding PO contents. Tribological properties proved that LDPE/GNP nanocomposites have lower coefficient of friction (COF) and wear rates in comparison with pure LDPE. By adding PO contents to the LDPE and its composites, COF and wear rates were gradually increased. Wear specimens' surfaces were imaged using scanning electron microscope.

✉ A. El-Sayed M. Hassan
a_sayed_hassan@yahoo.com

[1] Mechanical Department, Faculty of Industrial Education, Beni-Suef University, Beni-Suef, Egypt

[2] Composite Materials Laboratory, Advanced Materials Division, Central Metallurgical Research and Development Institute "CMRDI", Helwan, Cairo, Egypt

[3] Production Engineering and Mechanical Design Department, Faculty of Engineering, El-Minia University, El-Minia, Egypt

Keywords Low-density polyethylene · Paraffin oil · Graphene nanoplatelets · Mechanical properties · Tribological properties

1 Introduction

Nanocomposite materials with nanofiller have emerged in the last few decades as a promising class of materials, which take the advantage of greatly higher specific surface area, higher loads, and controlled interfacial interactions [1]. Conventional materials have been replaced with polymers in many applications, because of their low density, ease of processing, lightweight, low cost, corrosion resistance, and thermal insulation. Low-density polyethylene (LDPE), polypropylene (PP), polystyrene (PS), and many other polymers can be used in packaging applications [2–4]. Polymeric nanocomposite materials have solved many problems due to their extensive applications such as aerospace, automobiles, coatings, packaging materials, and construction engineering. Many researches have focused on the use of natural materials in the polymer nanocomposites as fillers [5,6]. Filler materials play an effective role in improvement in composite properties. Selecting size and shape of filler, filler types and loadings, optimum filler–matrix ratio, compatibility between matrix and filler interfacial bonds, and well filler distribution lead to improvement in the composite performance [7]. The uniform distribution of nanofiller in the polymer matrix can improve electrical, thermal, mechanical, flame-retardant, and gas barrier properties of the nanocomposite materials [5].

Nanofillers such as carbon nanofibres (CNFs), carbon nanotubes (CNTs), and exfoliated graphite (EG) are the most common fillers which are used for preparing the polymer nanocomposites [8,9]. Kuila et al. [5,10] found that CNTs are very effective conductive fillers in thermal, electrical, and

mechanical properties. However, CNTs have high production cost which limits their applications as nanofiller.

Graphene discovery in 2004 has largely overcome this problem [5]. Graphene is well known for its unique mechanical properties (tensile strength ∼ 130 GPa and elastic modulus ∼ 0.5–1 TPa), high specific surface area, and superior thermal and electrical properties [11]. These unique properties make graphene suitable for many applications in technological fields, including sensors, energy storage, electronic circuits, solar cells, and tribological applications [12–14]. In addition, one important application of graphene is using it as a reinforcement material in polymer matrix nanocomposites [15]. Recent studies, which conducted on the use of graphene as nanofiller, showed that it may be the best among other traditional nanofiller because of its unique properties [8].

The dispersion of graphene is an important factor to enhancement of polymer properties. There are three main blending techniques for the fabrication of polymer/graphene nanocomposites: melt mixing, solution blending, and in situ polymerization [16]. Among these three common techniques, melt mixing is the most eco-friendly and economical technique because it does not require any solvents and this process can be performed by using mechanical mixing machine such as extruder and internal mixer [17–20].

Generally, in the melt blending technique it is difficult to obtain well dispersion of graphene in polymer matrix without any pretreatment [21–23]. Solution blending is an effective technique to achieve homogeneous distribution of graphene in polymer [24–26], due to the ease of graphene processing and its derivatives in organic solvents [27,28].

The homogeneous dispersed graphene in polymer matrix can be achieved by another effective technique which is in situ polymerization [20,29]. The polymerization may take place between graphene layers or at graphene surface; in this case, in situ polymerization will not be suitable. The processability of nanocomposites may be reduced during polymerization because of the increased viscosity [30,31]. Between these three blending techniques, in situ polymerization showed better dispersion properties and good compatibility between the polymer and graphene because of the added functional groups to the graphene surface [30].

Improving the tribological properties of the polymeric composites can be achieved using nanofibres and nanoparticles [7]. Wear characteristics of polymer matrix nanocomposites are dependent on the materials properties and the sliding conditions, such as lubricating conditions, environment, and counterface materials [32]. Although many researches have been conducted on enhancing the tribological properties of polymer matrix nanocomposites by adding many fillers, there are few researches about reducing the wear of polymer composites by varying the sliding parameters [33].

Chang et al. [34,35] reported the tribological properties of short carbon fibre (SCF) /PA66 and SCF/epoxy polymer composites, and found that the composite properties were enhanced by adding 5 vol% of TiO_2 as a reinforcement nanoparticles. Incorporation of multi-walled carbon nanotubes (MWNT) in PP as a polymer matrix was studied by Dike et al. and showed an improvement in polypropylene wear resistance and mechanical properties. MWNTs with low filler concentrations showed a similar effect on wear resistance after adding to epoxy composites, in study done by Campo et al. [34]. Also, graphene oxide (GO) studies for reinforcement of polymer composites have proved that the tribological performance of polymeric matrices has been improved.

The incorporation of particulates and fibres within polymer matrix nanocomposites led to the formation of a uniform protecting transfer film on the abrasive counterface; therefore, the tribological performance could be improved. Also, load carrying capacity and strength of polymeric matrix will be increased. There are many studies carried out on using hybrid filler systems to enhance the performance of composites [35,36].

LDPE, which is within the polyethylene (PE) family, has attracted extensive attention in scientific studies due to the more flexible processing compared to high-density polyethylene (HDPE) and good balance between strength and rigidity [10,11]. PE could be blended with paraffins because of their structural and chemical similarities. These paraffins characterized by availability, stability, and low price [37]. Hence, some tribological studies emphasized on the adding of PO to the rubbing surfaces as a liquid lubricant [38,39].

The aim of the present work is to introduce new self-lubricating polymeric nanomaterials for light load-bearing applications and manufacture of fast and cheap polymeric dies. There have been some studies reported on improving the mechanical performance of LDPE/GNP composites [40–42]. However, there has been no study on the tribological performance of LDPE/GNP composites. Therefore, this work interested on studying the effect of different filler loadings of GNPs and PO, as a liquid lubricant, on the mechanical and tribological properties of LDPE nanocomposites.

2 Experimental Work

2.1 Materials

The matrix material, composed of powdered LDPE, was supplied from Saudi Arabia Basic Industries Corporation (SABIC), with an average particle size of 279.8 nm. This average particle size was identified by using zeta sizer nanoseries and was done at the Egyptian Petroleum Research Institute, Cairo, Egypt. GNPs, which were used

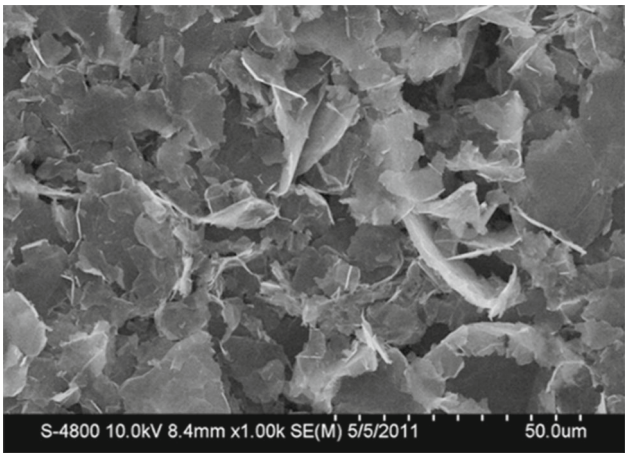

Fig. 1 SEM of as received GNPs

as a reinforcement material, having 2–10 nm thickness, 20–40 m^2/g specific surface area, and average particle diameter of $\sim$ 5 μm, were obtained from ACS MATERIALS Company, USA. Figure 1 shows the SEM image of GNPs. A medical grade of PO was used in the composites manufacturing at different loadings to study its effects on the mechanical and tribological properties of nanocomposites.

2.2 Nanocomposite Preparation

A hot compression technique at a compression pressure of 0.3 MPa was employed to produce the pure LDPE and its composites. Specimens were prepared as shown in Table 1, with the mass ratios (GNPs:LDPE) of 0, 0.25, 0.5, 0.75, and 1 weight fraction (wt%). All of these composites were fabricated with 0, 2.5, 5, 7.5, and 10 wt% of PO, whereas increasing PO level beyond 10 wt% in LDPE/GNPs resulted into poor mixing with the LDPE/GNP composite. The composites were mixed and heated for 10 minutes at temperature of 150 °C in a cylindrical pressing die. This pressing die was manufactured by M238 hot working steel, which has an internal diameter of 6.5 mm as shown in Fig. 2. After the temperature had reached to 135 °C, composites were hot pressed by a hydraulic pressing system as presented in Fig. 3. Then, specimens were cooled gradually to room temperature.

The cylindrical specimens having 6.5 mm diameter and 45 mm length were cut into suitable lengths, and these specimens were used for further testing.

2.3 Characterization Methods

Compression test was performed using SHIMADZU universal testing machine (UH series). The applied cross-head speed is 6 mm/min. The test was conducted at room temperature. The specimens were 6.5 mm in diameter and 13 mm in length according to ASTM D 695. Elastic modulus (stiffness)

Table 1 Specimens composition

Specimen no.	Specimens composition (wt%)		
	LDPE (wt%)	GNPs (wt%)	PO (wt%)
1	100	0	0
2	99.75	0.25	0
3	99.5	0.5	0
4	99.25	0.75	0
5	99	1	0
6	97.5	0	2.5
7	97.25	0.25	2.5
8	97	0.5	2.5
9	96.75	0.75	2.5
10	96.5	1	2.5
11	95	0	5
12	94.75	0.25	5
13	94.5	0.5	5
14	94.25	0.75	5
15	94	1	5
16	92.5	0	7.5
17	92.25	0.25	7.5
18	92	0.5	7.5
19	91.75	0.75	7.5
20	91.5	1	7.5
21	90	0	10
22	89.75	0.25	10
23	89.5	0.5	10
24	89.25	0.75	10
25	89	1	10

was calculated from slope of the engineering stress–strain curves, which resulted from the compression test.

Vickers microhardness test was conducted at room temperature according to ASTM E384-99. The specimens were 6.5 mm in diameter and 10 mm in length. The test was performed under an applied normal load of 50 g for 10 s. The size of the indentation was measured using a light microscope fixed with the testing machine.

In order to calculate the microhardness number, the applied normal load was divided by square of the mean diagonal length of the indentation. To find accurate results, at least five readings at different locations of samples were determined and average values were reported.

Figure 4 shows a pin-on-disc test rig used for sliding wear experiments. Wear test was conducted on the LDPE and its composites by using carbon steel disc to act as sliding counterface in accordance with the ASTM standard G99 [43]. The specimens were cut into pin shapes with dimensions of 6.5 mm in diameter and 30 mm in length. The steel disc has dimensions of 185 mm diameter, 8 mm thickness,

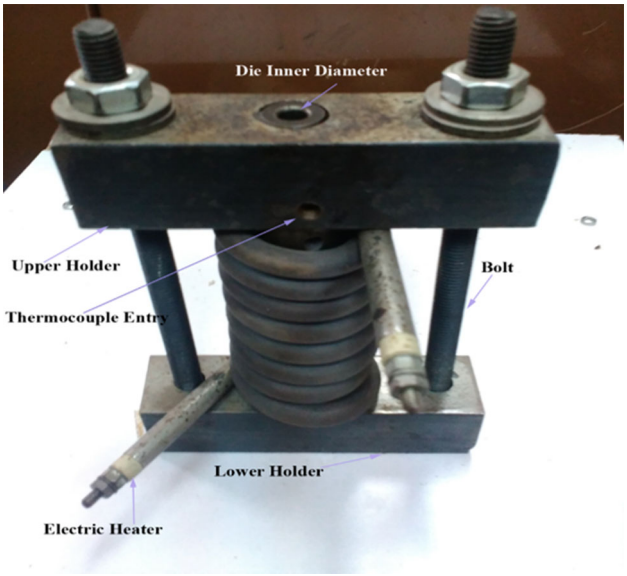

Fig. 2 Pressing die

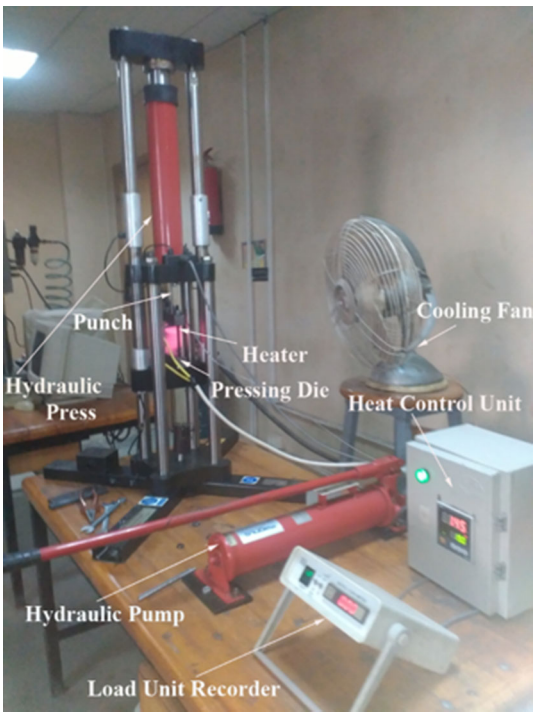

Fig. 3 Hydraulic pressing system

surface hardness of 58–62 HV, and surface roughness (Ra) of 1.11 μm. Wear test was performed on a track diameter of 150 mm for specified sliding distance, sliding speed, and applied normal load. The test was carried out at 30 ± 5 °C by an applied normal load of 20 N and run for a constant sliding distance and sliding speed of 212 m and 1.2 m/s, respectively. The values of normal load and sliding speed were selected keeping in view of the application of LDPE/GNP

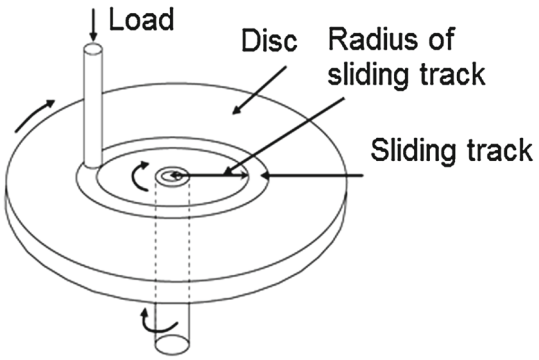

Fig. 4 Schematic diagram of pin-on-disc test rig

composite for light load bearings and polymeric dies. Specimens were weighed before and after the wear test using a digital electronic balance which has ± 0.1 mg accuracy. Difference between specimen weights represents the wear rate. The averaged values of at least three tests for each specimen were reported.

During the wear test, friction force was measured continuously throughout the wear test using a load cell of 40 kg. A load cell was connected to the calibrated data logger, which recorded the friction force each one millisecond, and their average values were introduced. The coefficient of friction was calculated by dividing the friction force by the applied normal force. The microstructure and worn surfaces of the composites were examined by SEM.

3 Results and Discussion

Figure 5 shows the results of compression test conducted on the pure LDPE and its composites with different loadings of PO (0, 2.5, 5, 7.5, and 10 wt%) and plotted in stress–strain curves to evaluate the behaviour and elastic modulus of composites under compression test.

Elastic modulus of LDPE/GNP nanocomposites showed gradually decreasing trend after addition of PO at contents of 2.5, 5, 7.5, and 10 wt%, as indicated in Fig. 6. This may be due to weak interaction between GNPs and LDPE, which leads to less effective stress transfer between LDPE and the reinforcement material.

According to the rule of mixtures, the modulus of elasticity is expected to increase with increasing GNP content. It is because of GNPs have high elastic modulus, high specific surface area, and the applied stress transferred from the LDPE to GNPs. Figure 6 shows that GNPs increased the elastic modulus of the pure LDPE by 34.61, 53.85, 57.25, and 83.31% at 0.25, 0.5, 0.75, and 1 wt% GNPs, respectively.

Figure 7 represents the microhardness measurements of the present LDPE/GNP/PO composites. It is clear that the microhardness of composites is higher than that of the non-

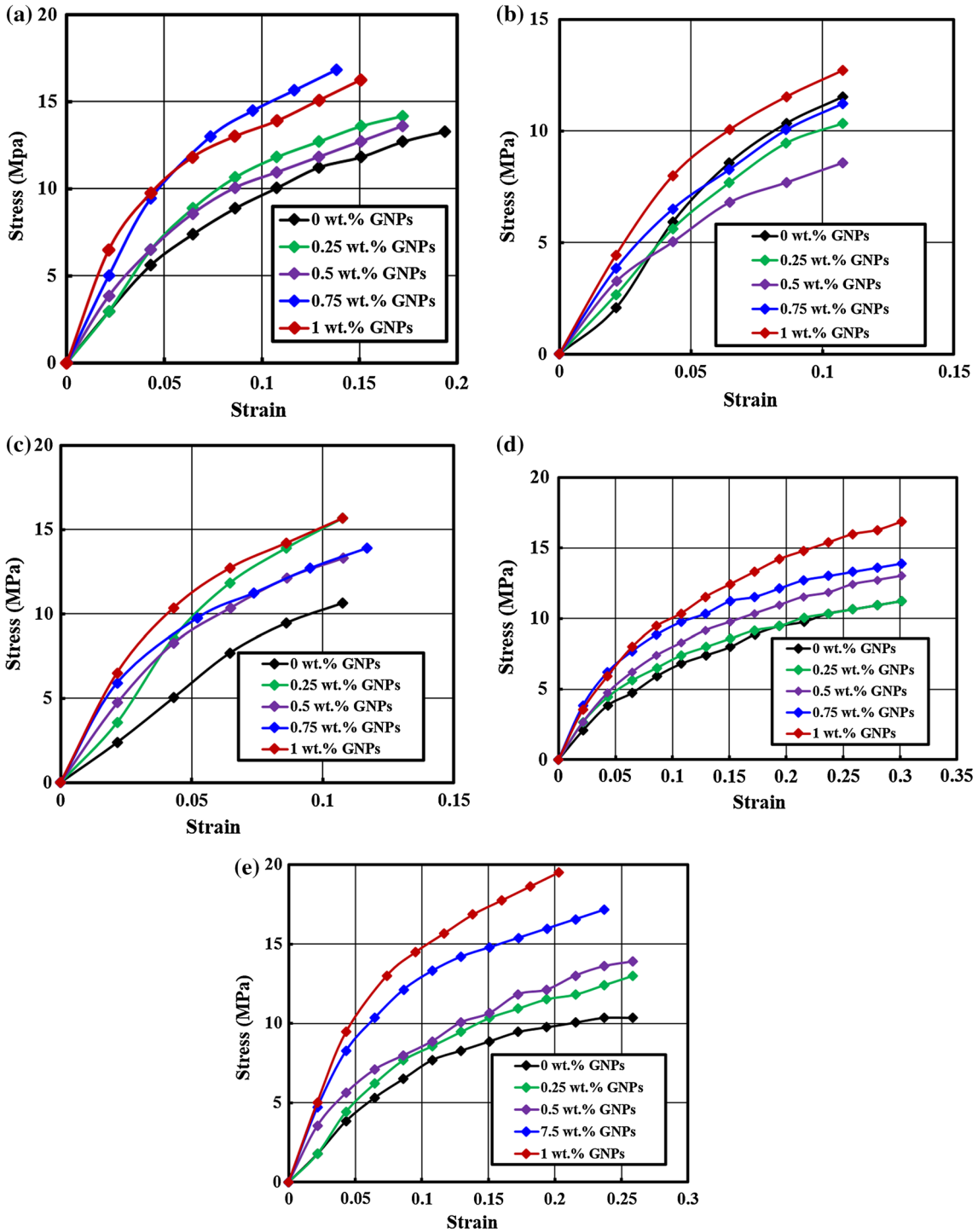

Fig. 5 Engineering stress strain curves of LDPE and its composites with different loadings of PO. **a** 0, **b** 2.5, **c** 5, **d** 7.5, and **e** 10 wt%

reinforced LDPE. GNPs increased the microhardness of the pure LDPE by 8.83, 23.89, 44.87, and 56.8% at 0.25, 0.5, 0.75, and 1 wt% loadings, respectively. The strong interfacial adhesion between the GNPs and LDPE matrix, and the molecular-level dispersion of GNPs in the matrix may be the reasons of the higher microhardness of the composites. Also, GNPs act as a strengthening material of the polymer matrix nanocomposites which contribute to improvement in load carrying capacity. After addition of PO to LDPE/GNP nanocomposites at loadings of 2.5, 5, 7.5, and 10 wt%, the microhardness of nanocomposites showed gradually decreasing trend. However, the microhardness of these

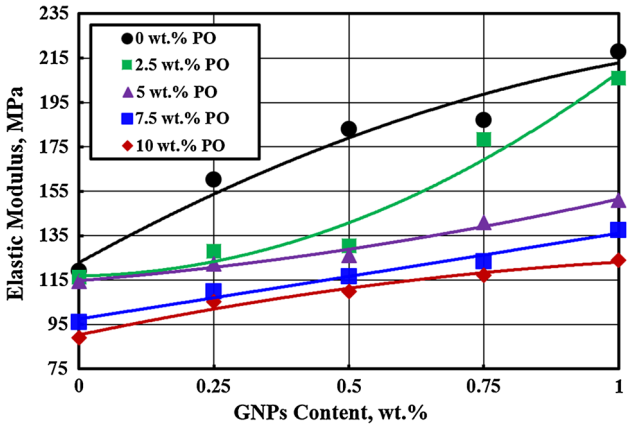

Fig. 6 Elastic modulus of different composites

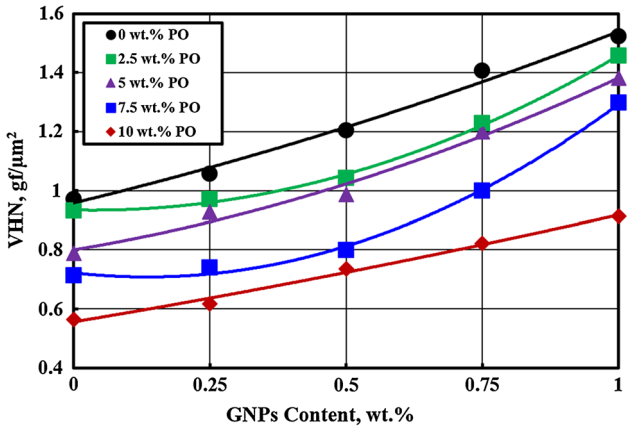

Fig. 7 Microhardness of different composites

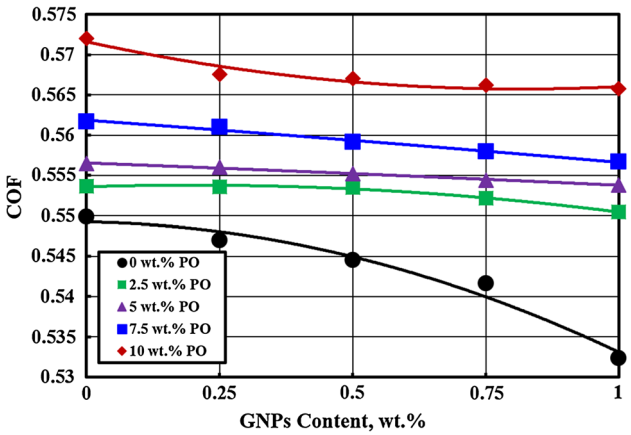

Fig. 8 COF of the tested composites

composites is still lower than that of composites without PO. All of the studied mechanical properties decreased as the PO content increased, which is attributed to that the mechanical properties of LDPE are higher than the mechanical properties of PO that has low molecular weight.

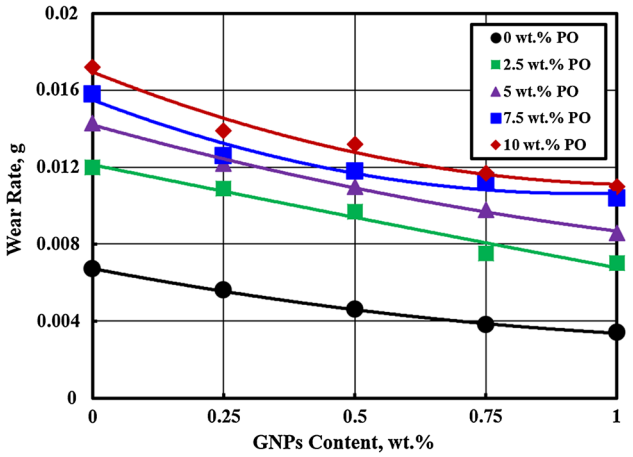

Fig. 9 Wear rate of the tested composites

The coefficient of friction (COF) and wear rate testing of pure LDPE and LDPE/GNP/PO nanocomposites were performed at a sliding speed of 1.2 m/s (150 rpm) and 20 N applied normal load, where the experimental results are introduced in Figs. 8 and 9, respectively. Figure 8 shows the COF results versus GNP wt% nanocomposites under dry sliding conditions. According to the friction coefficient variations as indicated in Fig. 8, GNPs reduced the COF of pure LDPE by 0.51, 0.97, 1.49, and 3.18% at 0.25, 0.5, 0.75, and 1 wt% GNP content, respectively. COF of the nanocomposites showed slightly decreasing trend by addition of GNPs. It is known that GNPs have a very low COF, so that adding GNPs into LDPE can obtain nanocomposites with a lower COF. On the other hand, GNPs can be readily dragged out from the polymeric matrix to form a third-body transfer film, which leads to reduce the direct contact between the polymeric matrix and counterpart. By adding PO of 2.5, 5, 7.5, and 10 wt% contents to the LDPE/GNP nanocomposites, COF increased gradually with increasing PO content. However, in all cases of PO contents, GNPs reduced the COF of LDPE/PO compared to pure LDPE and followed the same decreasing trend. This may be attributed to weak interaction between PO and LDPE/GNP composites and the emergence of porosity as indicated in SEM examination (Fig. 10d).

Figure 9 shows the wear rate as a function of GNPs wt% under dry sliding conditions. It is clear that unfilled LDPE records the highest wear rate compared to LDPE/GNP nanocomposites. Wear rate of LDPE was reduced by 16.42, 31.34, 43.28, and 49.25% at GNP contents of 0.25, 0.5, 0.75, and 1 wt%, respectively. The wear rate was lower with 1.0 wt% of GNPs. Generally, the LDPE/GNP nanocomposites exhibit decreased tendency of wear rate in dry sliding against the steel counterpart when the GNP content is increased. Because of high thermal conductivity and high strength of GNPs, the wear resistance has been improved due to transmission of frictional heat of nanocomposites

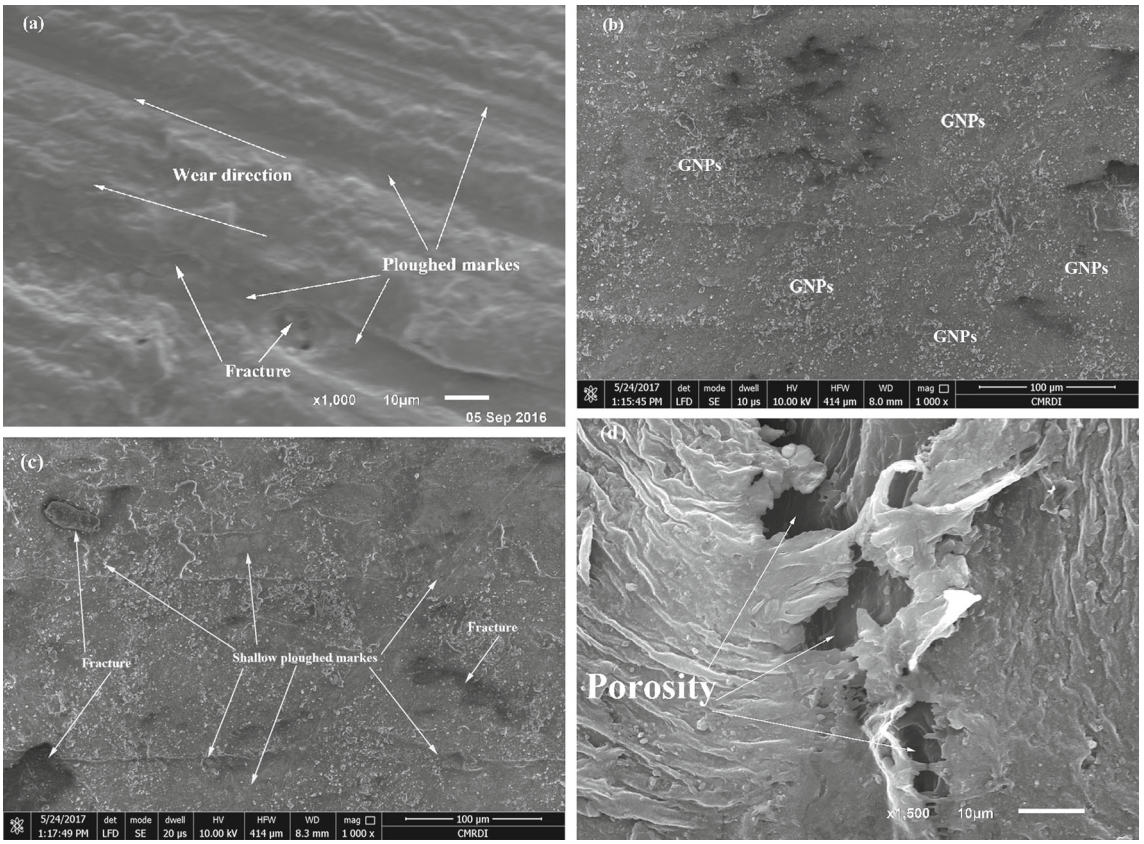

Fig. 10 SEM micrographs. **a** Worn surface of unfilled LDPE after wear, **b** distribution of 1 wt% GNPs in LDPE before wear, **c** worn surface of LDPE/1wt% GNPs after wear, and **d** worn surface of LDPE/1wt% GNPs/10 wt% PO after wear

and enhancement of the load carrying capacity [44]. After addition of PO to LDPE/GNP nanocomposites at contents of 2.5, 5, 7.5, and 10 wt%, the wear rate of nanocomposites showed gradually increasing trend compared with LDPE/GNP nanocomposites without PO. As known, there is a reverse relation between wear rate and hardness of nanocomposites. However, in all cases of PO contents, GNPs reduced the wear rate of LDPE/PO composites. In consideration of the low COF and wear rate, the LDPE/GNP nanocomposites of 1 wt% content could be a promising material for the tribological applications in dry sliding against steel.

Recent studies emphasized that this significant improvement in tribological performance of polymeric nanocomposites may be attributed to the transfer film formation, which protects the steel counterpart and specimens then leads to reducing the ability of wear rate and COF [31,45–47]. Composites with more uniform transfer films had lower COF and wear rates [47]. Hence, these transfer films were responsible for enhancement of the tribological performance of GNP-reinforced LDPE.

It may be considered that, at the start of a wear test, the specimen sliding surface comes in contact with the rough steel disc. The surface asperities of the steel disc have been adhered by transfer film, which was removed from the specimen surface under the influence of load and sliding speed. With the formation of uniform and coherent transfer film, a new stage begins where the sliding occurs between LDPE/GNP nanocomposites and the transfer film covering the steel disc surface. Consequently, low COF and wear rate have been obtained. Therefore, the GNPs play an important role in improving the wear resistance and reducing of COF of LDPE.

The comparison on the worn surfaces of unfilled LDPE, LDPE/1wt% GNPs, and LDPE/1wt% GNPs/10 wt% PO under constant sliding speed was characterized using SEM images as shown in Fig. 10.

As indicated in Fig. 10a, the worn surface of unfilled LDPE contains more ploughed marks, which illustrated that the wear mechanism was distinguished with adhesive and ploughing wear. Because of the increased temperature at contacted surfaces, severe adhesive wear occurred mainly due to the softening of unfilled LDPE. Moreover, the ploughed marks and fractures on the worn surfaces of the composites are caused by the microcutting and microploughing action from the abrasive asperities counterface.

Distribution of 0.25, 0.5, 0.75, and 1 wt% GNPs in LDPE matrix led to enhancement of the surface mechanical strength of LDPE. Figure 10b shows the distribution of 1wt% GNPs in LDPE matrix. The high surface mechanical strength of LDPE/1wt% GNP composites helps in preventing deeper wear grooves during sliding action. Besides surface properties, the transfer films formed during sliding also play a significant role in controlling the wear behaviour of the materials [7]. During the sliding process, these GNPs were easily released from the LDPE/GNP nanocomposites and transferred to the LDPE nanocomposite contact zone and the counterface. Thus, the GNPs could work as a solid lubricant material between the two contacted surfaces and prevent the direct contacting between them, thereby reducing the COF and increasing the wear resistance. This resulted in less wear marks and shallower grooves of LDPE/1wt% GNP worn surface, as shown in Fig. 10c. Hence, the LDPE/1wt% GNP nanocomposites showed much better friction and wear resistance compared with unfilled LDPE.

As for the worn surface of LDPE/1wt% GNPs filled with 10 wt% PO as shown in Fig. 10d, the porosity was shown clearly on the surface which led to weak interaction between the PO and LDPE/GNP nanocomposites. Therefore, increase in wear rate and COF with increasing PO content may be attributed to the porosity formation, which led to weak interaction between the PO and LDPE/GNP nanocomposites.

4 Conclusions

In the present study, LDPE matrix nanocomposites reinforced with GNPs and PO were fabricated and the mechanical and tribological properties of these nanocomposites were investigated. The elastic modulus and microhardness of LDPE were increased with increase in GNPs wt%, because GNPs act as a strengthening material of the LDPE matrix nanocomposites which contribute to improve the load carrying capacity. By adding PO wt%, the elastic modulus and microhardness of LDPE/GNP/PO nanocomposites were gradually decreased, due to the weak interaction, which caused by adding of PO. Wear rate and COF of LDPE were decreased with increase in GNPs wt%. This may be attributed to the high surface mechanical strength and the transfer film formation, which protects the steel counterface. Therefore, the GNPs play an important role in improving the wear resistance and reducing COF of LDPE. After addition of PO to LDPE/GNP nanocomposites at loadings of 2.5, 5, 7.5, and 10 wt%, the wear rate and COF of nanocomposites showed gradually increasing trend compared to LDPE/GNP nanocomposites without PO contents. This may be attributed to the weak interaction between PO and LDPE/GNP nanocomposites, and porosity formation was gradually increased. Finally, the worn surface was characterized using SEM to emphasize on the wear mechanism.

Acknowledgements This research was supported by production technology department in faculty of industrial education, Beni-Suef University, Egypt, and Composite Materials Lab, Central Metallurgical Research and Development Institute "CMRDI", Helwan, Cairo, Egypt.

References

1. Hu, K.; Kulkarni, D.D.; Choi, I.; Tsukruk, V.V.: Graphene-polymer nanocomposites for structural and functional applications. Prog. Polym. Sci. **39**(11), 1934–1972 (2014)
2. Luyt, A.S.; Geethamma, V.G.: Effect of oxidized paraffin wax on the thermal and mechanical properties of linear low-density polyethylene-layered silicate nanocomposites. Polym. Test **26**(4), 461–470 (2007)
3. Masjedi-Arani, M.; Ghanbari, D.; Salavati-Niasari, M.; Bagheri, S.: Sonochemical synthesis of spherical silica nanoparticles and polymeric nanocomposites. Clust. Sci. **27**(1), 25–38 (2016)
4. Cui, Y.; Kundalwal, S.I.; Kumar, S.: Gas barrier performance of graphene/polymer nanocomposites. Carbon **98**, 313–333 (2016)
5. Kuila, T.; Bose, S.; Mishra, A.K.; Khanra, P.; Kim, N.H.; Lee, J.H.: Effect of functionalized graphene on the physical properties of linear low density polyethylene nanocomposites. Polym. Test **31**(1), 31–38 (2012)
6. Verma, D.; Gope, P.C.; Shandilya, A.; Gupta, A.: Mechanical-thermal-electrical and morphological properties of graphene reinforced polymer composites: a review. Trans. Indian Inst. Met. **67**, 803–816 (2014)
7. Chang, B.P.; Akil, H.M.; Affendy, M.G.; Khan, A.; Nasir, R.B.M.: Comparative study of wear performance of particulate and fiber-reinforced nano-ZnO/ultra-high molecular weight polyethylene hybrid composites using response surface methodology. Mater. Des. **63**, 805–819 (2014)
8. Kuilla, T.; Bhadra, S.; Yao, D.; Kim, N.H.; Bose, S.; Lee, L.H.: Recent advances in graphene based polymer composites. Prog. Polym. Sci. **35**(11), 1350–1375 (2010)
9. Goodridge, R.D.; Shofner, M.L.; Hague, R.J.M.; McClelland, M.; Schlea, M.R.; Johnson, R.B.; Tuck, C.J.: Processing of a polyamide-12/carbon nanofibre composite by laser sintering. Polym. Test **30**(1), 94–100 (2011)
10. Kuila, T.; Bose, S.; Hong, C.E.; Uddin, M.E.; Khanra, P.; Kim, N.H.; Lee, J.H.: Preparation of functionalized graphene/linear low density polyethylene composites by a solution mixing method. Carbon **49**(3), 1033–1037 (2011)
11. Lahiri, D.; Hec, F.; Thiesse, M.; Durygin, A.; Zhang, C.; Agarwal, A.: Nanotribological behavior of graphene nanoplatelet reinforced ultra high molecular weight polyethylene composites. Tribol. Int. **70**, 165–169 (2014)
12. Kim, H.; Kobayashi, S.; AbdurRahim, M.A.; Zhang, M.J.; Khusainova, A.; Hillmyer, M.A.; Abdala, A.A.; Macosko, C.W.: Graphene/polyethylene nanocomposites: effect of polyethylene functionalization and blending methods. Polymer **52**(8), 1837–1846 (2011)
13. Das, T.K.; Prusty, S.: Graphene-based polymer composites and their applications. Polym. Plast. Technol. Eng. **52**(4), 319–331 (2013)
14. Vermisoglou, E.C.; Giannakopoulou, T.; Romanos, G.; Boukos, N.; Psycharis, V.; Lei, C.; Lekakou, C.; Petridis, D.; Trapalis, C.: Graphene-based materials via benzidine-assisted exfoliation and reduction of graphite oxide and their electrochemical properties. Appl. Surf. Sci. **392**, 244–255 (2017)

15. Zhang, H.B.; Zheng, W.G.; Yan, Q.; Yang, Y.; Wang, J.W.; Lu, Z.H.; Ji, G.Y.; Yu, Z.Z.: Electrically conductive polyethylene terephthalate/graphene nanocomposites prepared by melt compounding. Polymer **51**(5), 1191–1196 (2010)
16. Kalaitzidou, K.; Fukushima, H.; Drzal, L.T.: A new compounding method for exfoliated graphite-polypropylene nanocomposites with enhanced flexural properties and lower percolation threshold. Compos. Sci. Technol. **67**(10), 2045–2051 (2007)
17. Lee, J.H.; Kim, S.K.; Kim, N.H.: Effects of the addition of multi-walled carbon nanotubes on the positive temperature coefficient characteristics of carbon-black-filled high-density polyethylene nanocomposites. Scr. Mater. **55**(12), 1119–1122 (2006)
18. Sengupta, R.; Bhattacharya, M.; Bandyopadhyay, S.; Bhowmick, A.K.: A review on the mechanical and electrical properties of graphite and modified graphite reinforced polymer composites. Prog. Polym. Sci. **36**(5), 638–670 (2011)
19. Kim, H.; Macosko, C.W.: Processing-property relationships of polycarbonate/graphene composites. Polymer **50**(15), 3797–3809 (2009)
20. Steurer, P.; Wissert, R.; Thomann, R.; Mulhaupt, R.: Functionalized graphenes and thermoplastic nanocomposites based upon expanded graphite oxide. Macromol. Rapid Commun. **30**(4–5), 316–327 (2009)
21. Fu, S.; Li, N.; Wang, K.; Zhang, Q.; Fu, Q.: Reduction of graphene oxide with the presence of polypropylene micro-latex for facile preparation of polypropylene/graphene nanosheet composites. Colloid Polym. Sci. **293**, 1495–1503 (2015)
22. Stankovich, S.; Dikin, A.D.; Dommett, G.H.B.: Graphene-based composite materials. Nature **442**(7100), 282–286 (2006)
23. Liang, J.; Huang, Y.; Zhang, L.; Wang, Y.; Ma, Y.; Guo, T.; Chen, Y.: Molecular-level dispersion of graphene into poly(vinyl alcohol) and effective reinforcement of their nanocomposites. Adv. Funct. Mater. **19**(14), 2297–2302 (2009)
24. Zhou, T.; Zhou, F.; Tang, C.; Bai, H.; Zhang, Q.; Deng, H.; Fu, Q.: The preparation of high performance and conductive poly (vinyl alcohol)/graphene nanocomposite via reducing graphite oxide with sodium hydrosulfite. Compos. Sci. Technol. **71**(9), 1266–1270 (2011)
25. Zhan, Y.; Wu, J.; Xia, H.; Yan, N.; Fei, G.; Yuan, G.: Dispersion and exfoliation of graphene in rubber by an ultrasonically-assisted latex mixing and in situ reduction process. Macromol. Mater. Eng. **276**(7), 590–602 (2011)
26. Bai, X.; Wan, C.; Zhang, Y.; Zhai, Y.: Reinforcement of hydrogenated carboxylated nitrile-butadiene rubber with exfoliated graphene oxide. Carbon **49**(5), 1608–1613 (2011)
27. Du, J.; Cheng, H.: The fabrication, properties, and uses of graphene/polymer composites. Macromol. Chem. Phys. **213**(10–11), 1060–1077 (2012)
28. Verdejo, R.; Bernal, M.M.; Romasanta, L.J.; Lopez, M.A.: Graphene filled polymer nanocomposites. Mater. Chem. **21**(10), 3301–3310 (2010)
29. Kim, H.; Abdala, A.A.; Macosko, C.W.: Graphene/polymer nanocomposites. Macromolecules **43**(16), 6515–6530 (2010)
30. Yoo, B.M.; Shin, H.J.; Yoon, H.W.; Park, H.B.: Graphene and graphene oxide and their uses in barrier polymers. J. Appl. Polym. Sci. **131**(1), 1–23 (2014)
31. Chang, B.P.; Akil, H.M.; Nasir, R.B.; Khan, A.: Optimization on wear performance of UHMWPE composites using response surface methodology. Tribol. Int. **88**, 252–262 (2015)
32. Chang, L.; Zhang, Z.; Breidt, C.; Friedrich, K.: Tribological properties of epoxy nanocomposites I. Enhancement of the wear resistance by nano-TiO_2 particles. Wear **258**(1–4), 141–148 (2005)
33. Li, C.; Friedrich, L.: Enhancement effect of nanoparticles on the sliding wear of short fiber-reinforced polymer composites: a critical discussion of wear mechanisms. Tribol. Int. **43**(12), 2355–2364 (2010)
34. Campo, M.; Jiménez-Suárez, A.; Ureña, A.: Effect of type, percentage and dispersion method of multi-walled carbon nanotubes on tribological properties of epoxy composites. Wear **324**, 100–108 (2015)
35. Chunying, M.; Peng, N.; Jie, S.H.; Zhaozhu, Z.; Kaili, Z.: Study of tribological properties of polyimide/graphene oxide nanocomposite films under seawater-lubricated condition. Tribol. Int. **80**, 131–140 (2014)
36. Tai, Z.; Chen, Y.; An, Y.; Yan, X.; Xue, Q.: Tribological behavior of UHMWPE reinforced with graphene oxide nanosheets. Tribol. Lett. **46**, 55–63 (2012)
37. Krupa, I.; Nógellová, Z.; Špitalský, Z.; Malíková, M.; Sobolciak, P.; Abdelrazeq, H.; Ouederni, M.; Karkri, M.; Janigová, I.; Al-Maadeed, M.: Positive influence of expanded graphite on the physical behavior of phase change materials based on linear low-density polyethylene and paraffin wax. Thermochim. Acta **614**, 218–225 (2015)
38. Zhang, Z.; Xue, Q.; Liu, W.; Shen, W.: Friction and wear properties of metal powder filled PTFE composites under oil lubricated conditions. Wear **210**, 151–156 (1997)
39. Jia, B.; Li, T.; Liu, X.; Cong, P.: Tribological behaviors of several polymer–polymer sliding combinations under dry friction and oil-lubricated conditions. Wear **262**, 1353–1359 (2007)
40. Lei, H.; Liu, Z.; He, C.; Zhang, S.; Liu, Y.; Hua, C.; Li, X.; Li, F.; Chen, C.; Cai, R.: Graphene enhanced low-density polyethylene by pretreatment and melt compounding. RSC Adv. **6**, 101492–101500 (2016)
41. Fim, F.; Basso, N.; Graebin, A.; Azambuja, D.; Galland, G.: Thermal, electrical, and mechanical properties of polyethylene-graphene nanocomposites obtained by in situ polymerization. J. Appl. Polym. Sci. **128**, 2630–2637 (2013)
42. Gaska, K.; Gubanski, X.; Kádár, G.: Electrical, mechanical, and thermal properties of LDPE graphene nanoplatelets composites produced by means of melt extrusion process. Polymers **9**, 30–40 (2017)
43. Şahin, Y.: Analysis of abrasive wear behavior of PTFE composite using Taguchi's technique. Cogent Eng. **1**, 1–15 (2015)
44. Pan, B.; Zhang, S.; Li, W.; Zhao, J.; Liu, J.; Zhang, Y.; Zhang, Y.: Tribological and mechanical investigation of MC nylon reinforced by modified graphene oxide. Wear **294**, 395–401 (2012)
45. Guo, F.; Zhang, Z.; Liu, W.; Su, F.; Zhang, H.: Influence of solid lubricant reinforcement on wear behavior of Kevlar fabric composites. Appl. Polym. Sci. **110**, 1771–1777 (2008)
46. Li, Y.; Wang, Q.; Wang, T.; Pan, G.: Preparation and tribological properties of graphene oxide/nitrile rubber nanocomposites. J. Mater. Sci. **47**, 730–738 (2012)
47. Liu, H.; Li, Y.; Wang, T.; Wang, Q.: In situ synthesis and thermal, tribological properties of thermosetting polyimide/graphene oxide nanocomposites. J. Mater. Sci. **47**, 1867–1874 (2012)